JOURNAL OF VIROLOGY, Mar. 1993, p. 1357–1364
0022-538X/93/031357-08$02.00/0

Vol. 67, No. 3

Mutations in Herpes Simplex Virus Type 1 Genes Encoding VP5 and VP23 Abrogate Capsid Formation and Cleavage of Replicated DNA

PRASHANT DESAI, NEAL A. DELUCA, JOSEPH C. GLORIOSO, AND STANLEY PERSON*

Department of Molecular Genetics and Biochemistry, University of Pittsburgh, Pittsburgh, Pennsylvania 15261

Received 18 September 1992/Accepted 14 December 1992

The herpes simplex virus type 1 capsid is composed of seven capsid proteins which are termed VP5, VP19c, VP21, VP22a, VP23, VP24, and VP26. Major capsid protein VP5 is encoded by the gene *UL19*. *UL18*, whose transcript is 3′ coterminal with that of VP5, specifies capsid protein VP23. Vero cell lines have been isolated that are transformed with either the *Bgl*II N (*UL19*) or *Eco*RI G (*UL16* to *UL21*) fragment of KOS. These cell lines, selected for the ability to support the replication of a temperature-sensitive VP5 mutant, were used to isolate VP5 and VP23 null mutants. The mutations in VP5 (K5ΔZ) and VP23 (K23Z) were generated by insertion of the *lacZ* gene at the beginning of the coding sequences of the genes. Both mutants failed to form plaques on the nonpermissive cell line, and therefore, VP23, like VP5, is an essential gene product for virus replication. Both mutants expressed wild-type levels of infected-cell proteins upon infection of permissive and nonpermissive cell lines. However, the VP5 (150-kDa) and VP23 (33-kDa) polypeptides were absent in lysates prepared from K5ΔZ- and K23Z-infected Vero cells, respectively. No capsid structures were observed by electron microscopic analysis of thin sections of K5ΔZ- and K23Z-infected Vero cells. Following sedimentation of lysates from cells infected by the mutants, capsid proteins were not observed in the fractions where capsids normally sediment. The amounts of DNA replicated in the VP5 and VP23 mutant and in KOS-infected Vero cells were the same as in permissive cells. However, genomic ends were not evident in Vero cells infected with the mutants, suggesting that the DNA remains in concatemers and is not processed into unit length genomes.

The herpes simplex virion is comprised of four distinct components, the core, capsid, tegument, and envelope. The electron-dense core contains the viral nucleic acid. An icosahedral capsid structure encloses this core. An amorphous layer termed the tegument surrounds the capsid, and the tegument is enveloped by a lipid membrane in which are embedded the virus glycoproteins. The assembly of the capsid is therefore an essential step in virion morphogenesis. The herpes simplex virus type 1 (HSV-1) capsid is an icosahedral shell (42) which is composed of seven proteins, VP5 (150 kDa), VP19c (50 kDa), VP21 (43 kDa), VP22a (40 kDa), VP23 (33 kDa), VP24 (24 kDa), and VP26 (12 kDa) (9, 14, 16). There are approximately 900 molecules of VP5 per capsid for equine herpes virus 1 (24) and a similar number for HSV-1. Relative to 900 molecules of VP5 per capsid, there are approximately 1,400 of VP26, 900 of VP22a, 700 of VP19c, 400 of VP23, and 100 each of VP21 and VP24 (22–24).

Three types of capsids can be isolated from HSV-1-infected cells. Capsids are visualized as light-scattering bands in sucrose gradients and are designated A, B, and C, in order of increasing distance sedimented (14). These differ in protein and nucleic acid composition and in their eventual fate in infected cells. A and C capsids are similar in protein composition, but only C capsids contain viral DNA. B capsids differ from A and C capsids in that B capsids contain an abundant VP22a protein inside the shell. VP22a is intimately involved in the packaging of viral DNA (27, 33, 38). VP22a may function by forming a scaffold in the inner capsid space, and acquisition of DNA results in concomitant loss of VP22a from the capsid shell (4, 23). Conceptually, B capsids may be the precursors to C capsids in the viral assembly pathway, while A capsids may result from abortive attempts at DNA packaging.

The capsid shell is made up of 162 capsomeres (42) showing icosahedral symmetry of triangulation class T=16. For this class, 12 capsomeres are pentavalent (pentons) and the rest are hexavalent (hexons) (see, for example, references 4, 13, and 36). VP5, which represents 60% of the capsid mass, is the major component of the hexons and may also form the penton structures (31, 40). The spatial distribution of the other capsid proteins is largely unknown. Hexamers are connected on the outer surface by Y-shaped structures, and these maybe composed of VP26, as suggested by Baker et al. (4). Minor proteins (VP21 and VP24) may account for pentons or special capsid functions such as acquisition of DNA during virus replication and release of DNA following penetration of the virus into an infected cell. VP5 extends from the outside to the inside of the capsid and must engage in interactions with itself to form hexamers and with the other major proteins (VP19c, VP23, and VP26) to form the complete capsid (4, 13, 31, 36). VP19c binds HSV-1 DNA and forms one or more covalent disulfide bonds with VP5 (6, 43). DNA is packaged within the central region of the capsid, occupying the entire space out to the beginning of the capsid shell (5).

The functions and properties of the capsid proteins are unclear. Temperature-sensitive (*ts*) lesions in the genes that encode VP5 (29, 41) and VP19c (26) result in the absence of mature capsids at the nonpermissive temperature. *UL26* encodes a family of related proteins, including VP22a, which

* Corresponding author.

are processed after translation (18–20, 27, 28). Temperature-sensitive mutants for *UL26* gene products synthesize viral DNA and B capsids at the nonpermissive temperature but are unable to package this DNA to produce C capsids (33, 38).

The overall goal of our work is to construct null mutants for all of the capsid genes to identify the steps in the assembly of HSV-1 capsids and to characterize the role of each protein in this process. Null mutants are desirable since they allow comparisons to be made in the presence and in the complete absence of each protein. Complications due to transdominant effects of mutant polypeptides are also avoided. The capsid proteins are expected to be essential for virus replication on the basis of the finding that *ts* mutations have been mapped to genes that specify VP5, VP19c, and VP22a (26, 27, 41). Therefore, transformed cell lines that express these genes in *trans* are required for propagation of mutant viruses. In this report, we describe the isolation of transformed cell lines that express VP5 and VP23, which are encoded by genes *UL19* and *UL18*, respectively (10, 39). Furthermore, we have isolated and initiated the characterization of null mutants for these genes.

MATERIALS AND METHODS

Cells and viruses. Human embryonic lung (HEL) cells were grown and maintained as described by Person et al. (25). Vero cells and the E43 and G5 transformed cell lines were grown in Eagle's minimum essential medium supplemented with 10% fetal calf serum (GIBCO-BRL) and passaged as were HEL cells. Virus stocks of KOS (HSV-1) and of the VP5 (K5ΔZ) and VP23 (K23Z) null mutants were prepared as previously described (25). The KOS isolate used was passaged twice from the P17 stock obtained from Priscilla A. Schaffer (Harvard University) in 1973. G5 was used as the permissive cell line for propagation of the null mutants and gave yields of approximately 200 PFU per cell.

Plasmids. The *Eco*RI G (16.2-kb) and *Bgl*II N (5.7-kb) fragments of KOS were cloned into the *Eco*RI site of pUC9 and the *Bam*HI site of pUC19 and were designated pKEG and pKBgN, respectively (see Fig. 1). Plasmids are designated as to the source of viral DNA (K for the KOS strain) and as to the restriction fragment, EG for the G fragment of restriction endonuclease *Eco*RI. A null mutation in VP5 was generated first by partial digestion of pKBgN with *Nco*I, which deleted 1.8 kb; this was followed by ligation with a 10-bp *Bgl*II linker (see Fig. 2A). The *lacZ* gene, derived as a *Bam*HI cassette from pSC8 (8), was then cloned into the *Bgl*II site. This cassette does not contain an initiation codon but does have a TAA termination codon. The construction of a VP23 null mutation was initiated by subcloning a 1.1-kb *Pvu*I-*Stu*I fragment into *Sma*I-*Hin*cII-cut pUC19 after blunt ending the *Pvu*I site with T4 DNA polymerase (see Fig. 2B). This clone contains approximately 500 bp of the sequences both upstream and downstream of the VP23 initiation codon (20). The plasmid was cut with *Nru*I, which cuts in the 11th codon of VP23, and a 10-bp *Xho*I linker was inserted to create pKPSX. The *lacZ* sequence from pSC8 was obtained as an *Xho*I cassette and cloned into the *Xho*I site of pKPSX such that expression of LacZ initiates at the VP23 ATG and the protein is synthesized fused in frame with the first 10 codons of VP23.

Antibodies. Monoclonal antibody LP12 directed to VP5 was a kind gift from Anthony C. Minson (University of Cambridge). Polyclonal rabbit serum CP3 was prepared against VP23 isolated by preparative sodium dodecyl sulfate-polyacrylamide gel electrophoresis (SDS-PAGE) of purified B capsids. This serum was prepared by East Acres Biologicals. Capsids were purified by sedimentation of infected-cell lysates through 20 to 50% sucrose gradients.

Construction of transformed Vero cell lines. The procedure of DeLuca et al. (11) was followed for transformation of Vero cells. Subconfluent monolayers of Vero cells (2×10^6) in 100-mm-diameter petri dishes were cotransfected with pSV2neo (1.5 μg) (35) and either pKBgN (5 μg) or pKEG (30 μg) by using the calcium precipitation procedure of Graham and Van der Eb (15). At 24 h after transfection, the cells were harvested and plated at a density of 4×10^5/100-mm dish in medium containing 1 mg of G418 (GIBCO-BRL) per ml. The medium was replenished every 3 days. G418-resistant colonies were harvested by using Perspex cloning chambers and tested for the ability to support the replication of *ts*1178 (41). Positive isolates were colony purified twice and then further characterized. Cell line E43 was transformed with the *Bgl*II N fragment, and G5 was transformed with the *Eco*RI-G sequence.

Marker transfer of null mutations. Subconfluent monolayers of E43 or G5 cells in 60-mm dishes were cotransfected with 2 μg of a linearized plasmid and 10 μg of KOS genomic DNA extracted from crude virion preparations. The calcium precipitation technique of Graham and Van der Eb was used with the dimethyl sulfoxide enhancement modification of Stow and Wilkie (37). When foci were observed (48 h after transfection), the cell monolayers were harvested, freeze-thawed once, and sonicated and the titer of the total virus progeny was determined. To isolate viruses that expressed β-galactosidase, plaques were allowed to form under methylcellulose for 48 h after infection. This overlay was replaced with 1% low-melting-point agarose in medium containing 300 μg of Bluo-gal (GIBCO-BRL) per ml. Plaques that stained blue were picked and further plaque purified three times by limiting dilution in 96-well trays.

Southern blot hybridization. DNA sequences were detected after agarose electrophoresis as described by Southern (34), by using random-primer-labelled probes (12).

Sedimentation analysis. HEL cells (3×10^7) were infected at a multiplicity of infection (MOI) of 10 PFU per cell. At 6 h after infection, the monolayers were washed twice with tricine-buffered saline (25), methionine-free medium containing 750 μCi of [^{35}S]methionine (NEN-DuPont) was added, and the mixture was incubated for a further 6 h. The cells were washed once with tricine-buffered saline, harvested, and pelleted at 3,500 × *g* for 15 min at 4°C. The cell pellet was suspended in capsid lysis buffer (500 mM NaCl, 20 mM Tris [pH 7.5], 1 mM EDTA [pH 8.0], 1% Triton X-100, 0.5 mM tosyl lysyl chloromethyl ketone) and left on ice for 5 min, and the nuclei were pelleted by centrifugation at 3,500 × *g* for 30 min at 4°C. The resulting nuclei were freeze-thawed three times and sonicated, and the DNA was sheared by being passed through a 26.5-gauge needle several times. The nuclear lysate was layered onto a 20 to 50% (wt/wt) sucrose gradient (in 300 mM NaCl, 20 mM Tris [pH 7.5], 1 mM EDTA [pH 8.0], 0.5 mM tosyl lysyl chloromethyl ketone) and centrifuged at 24,000 rpm for 100 min in a Beckman SW41 rotor at 4°C. Fractions were collected and precipitated with an equal volume of 16% trichloroacetic acid. The trichloroacetic acid-precipitated protein was resuspended in sample buffer, and a fraction of this was analyzed by SDS-PAGE.

Immunoprecipitation and SDS-PAGE. Radiolabelling of infected cells, immunoprecipitation of antigen, and SDS-

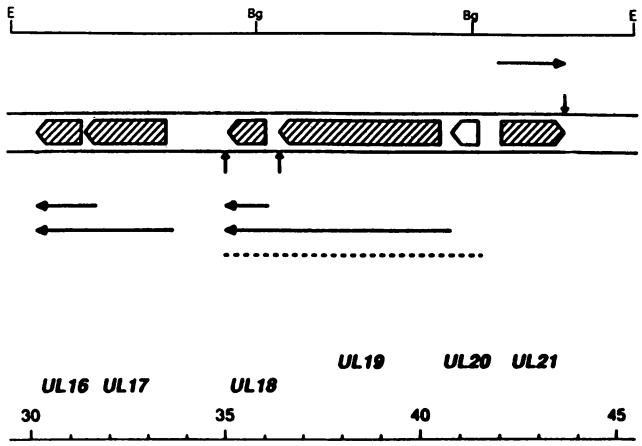

FIG. 1. The *Eco*RI-G region of the KOS genome. The 16.2-kb *Eco*RI G fragment was cloned into pUC9. Restriction sites are shown in the top line for *Bgl*II (Bg) and *Eco*RI (E). The remainder of the figure is from sequence analyses of HSV-1 strain 17 (20, 21). ORFs and directions of translation are as indicated, as are transcripts (←) and polyadenylation signals (↑). Nucleotide numbers from the left end of the strain 17 genome are given at the bottom in kilobases. The *Eco*RI G fragment specifies genes *UL16* through *UL21*. *UL18* and *UL19* encode two of the capsid proteins, VP23 and VP5, respectively. The *Bgl*II N fragment of KOS specifies only the *UL19* gene. The transcripts were mapped by Costa et al. (10).

PAGE analyses were performed as described by Cai et al. (7).

RESULTS

Isolation of transformed cell lines expressing capsid genes. The capsid gene products are essential for virion morphogenesis, and therefore a prerequisite for the isolation of null mutants for these genes is construction of transformed cell lines that express these genes in *trans*. Vero cells were therefore cotransfected with pSV2neo (35) and plasmids that express only *UL19* (pKBgN) or genes *UL16* through *UL21* (pKEG) (Fig. 1) (21). Colonies that were resistant to the drug G418 were harvested and tested for the ability to complement the lesion in *ts*1178. This mutant is a member of the G complementation group, and the lesion in it has been mapped to the VP5 locus (29, 41). Cell lines that tested positive for complementation were colony purified twice and then characterized further. Cell lines E43 and G5 were transformed with the *Bgl*II-N and *Eco*RI-G sequences, respectively. The cell lines were tested for the ability to support the growth of *ts*1178 at 34 and 39°C. E43 gave a plaquing efficiency for *ts*1178 (39/34°C) of 62%, and G5 gave a plaquing efficiency of 80% (Table 1). E43 was used as the permissive cell line for isolation of a VP5 null mutant. G5 was used to isolate a VP23 null mutant and to propagate both

TABLE 1. Complementation of *ts*1178 by transformed Vero cells

Cell type	Plating efficiency of *ts*1178[a] at:		
	34°C (PFU/ml)	39°C (PFU/ml)	39/34°C (%)
Vero	2.1×10^{10}	6.5×10^{6}	0.031
E43	1.2×10^{10}	7.5×10^{9}	62
G5	2.5×10^{10}	2.0×10^{10}	80

[a] The data shown are averages of two experiments.

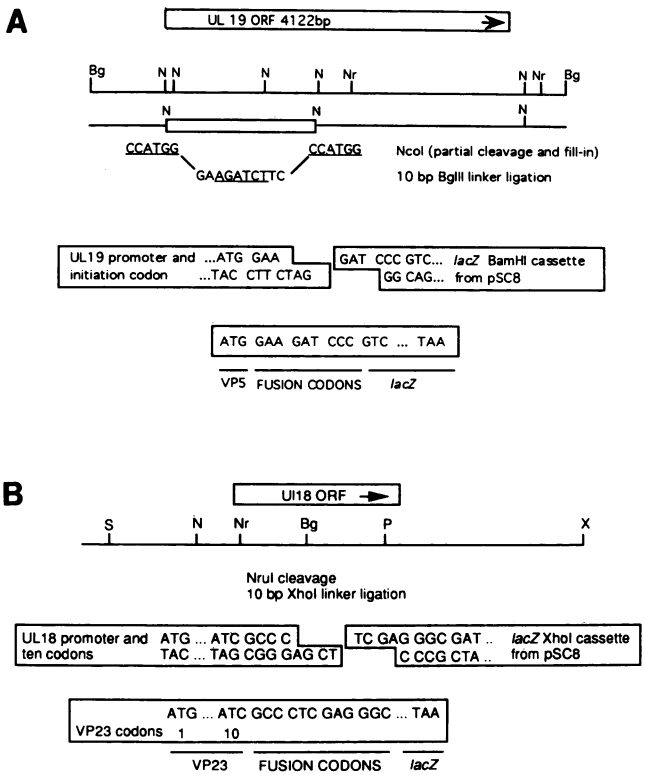

FIG. 2. Construction of *UL19* and *UL18* null mutation plasmids by insertion of a *lacZ* cassette. (A) The *UL19* ORF is depicted at the top in the left-to-right orientation. Immediately underneath is the *Bgl*II N fragment of KOS that was cloned into the *Bam*HI site of pUC19. The five *Nco*I sites are shown (N). A 1.8-kb *Nco*I deletion was constructed by a partial digest. The *UL19* start codon is within the most 5′ *Nco*I site. Following a fill-in reaction, a 10-bp *Bgl*II (Bg) linker was added at the site of the deletion. The resulting plasmid was digested with *Bgl*II, and the *Bam*HI *lacZ* cassette from pSC8 (8) was introduced in the orientation indicated. (B) The *UL18* ORF is illustrated together with a map of restriction sites in this gene and the surrounding sequences. A 1.1-kb *Pvu*I (P)-to-*Stu*I (S) fragment was cloned into the *Sma*I-*Hin*cII sites of pUC19 after treating the *Pvu*I end with T4 DNA polymerase. A 10-bp *Xho*I (X) linker was inserted into the *Nru*I (Nr) site of this plasmid. *Nru*I cleaves this sequence in codon 11 of *UL18*. An *Xho*I *lacZ* cassette derived from pSC8 was then cloned into this *Xho*I site.

mutants. Virus stocks of the VP5 null mutant prepared on E43 cells gave lower titers and smaller plaques than when G5 was used. Chromosomal DNA extracted from G5 was analyzed by Southern blot hybridization using the *Eco*RI G fragment as a probe. A 16-kb fragment was detected in G5 DNA, and this was present at 10 to 20 copies per cell (data not shown).

Construction and isolation of VP5 and VP23 mutants. The goal of these experiments was to construct mutations in the VP5 and VP23 genes and transfer these into the KOS genome by using E43 and G5 as permissive host cells. To construct the VP5 mutation, the 5.7-kb *Bgl*II N fragment was subcloned into the *Bam*HI site in pUC19 (Fig. 2). Figure 2A depicts the *UL19* (VP5) open reading frame (ORF) in the left-to-right orientation. *Bgl*II-N of KOS contains five *Nco*I sites, and the most 5′ site contains within it the ATG initiation codon of VP5 (20). Partial *Nco*I digestion was used to cleave at three of these sites, and this step resulted in a

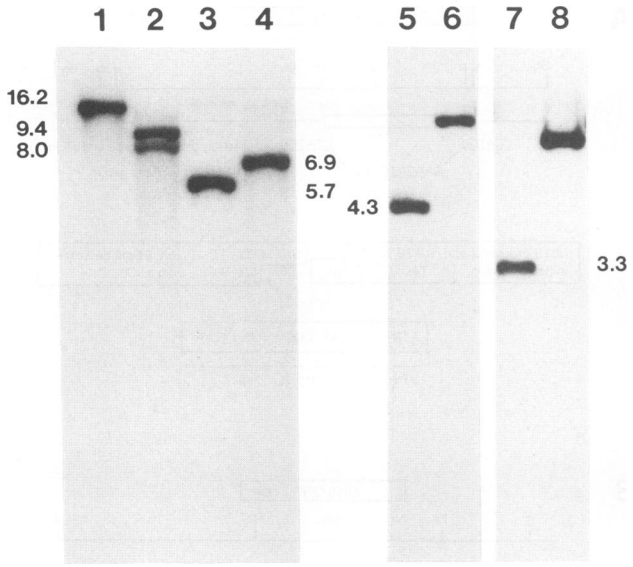

FIG. 3. Southern blot analysis of VP5 and VP23 null mutants. DNAs (2 μg) extracted from KOS (lanes 1, 3, 5, and 7)-infected Vero cells and K5ΔZ (lanes 2 and 4)- and K23Z (lanes 6 and 8)-infected G5 cells were digested with restriction endonucleases *Eco*RI (lanes 1 and 2), *Bgl*II (lanes 3 and 4), *Stu*I (lanes 5 and 6), and *Sal*I (lanes 7 and 8). The resulting restriction fragments were separated on a 1% agarose gel and transferred to nitrocellulose. Filters were hybridized to a ^{32}P-labelled probe corresponding to *Bgl*II-N (lanes 1 to 4) sequences or the 1.1-kb *Pvu*I-*Stu*I (lanes 5 to 8) fragment. The numbers beside the lanes indicate molecular sizes in kilobases.

deletion of 1.8 kb. The deletion was created so that the length of the resulting transcript would not be much greater than that of wild-type VP5. In addition, partial cleavage was employed because of a concern that the sequence between the fourth and the fifth sites contains the VP23 promoter element. There is also a polyadenylation signal at the end of the *UL19* ORF which may be utilized by *UL19* and/or *UL20*. The 5′ *Nco*I site was filled in, and a 10-bp *Bgl*II linker was added. Finally, the *lacZ* gene, derived as a *Bam*HI cassette from pSC8 (8), was introduced into the *Bgl*II site in the orientation shown. The *lacZ* gene utilizes the VP5 promoter and initiation codon. The LacZ polypeptide in this construct starts at its ninth codon (GTG) and is preceded by three fusion codons. Translation termination occurs at the LacZ TAA codon. The VP23 gene (*UL18*) (39) contains at its 10th and 11th codons an *Nru*I site which was used to insert the *lacZ* gene (Fig. 2B). A 1.1-kb *Stu*I-to-*Pvu*I fragment was cloned into the *Sma*I-*Hin*cII sites of pUC19. A 10-bp *Xho*I linker was introduced into the *Nru*I site, and the *lacZ* gene, obtained as an *Xho*I cassette from pSC8, was cloned into this site such that expression of this gene is driven by the *UL18* promoter and the LacZ polypeptide is synthesized as a fusion product containing the first 10 codons of VP23. Expression of LacZ was used to screen for mutant viruses by virtue of their ability to form blue plaques when overlaid with Bluo-gal in cotransfection experiments.

Linearized plasmid DNA and intact KOS DNA were used to cotransfect E43 or G5 cells. Progeny virus was harvested and assayed for the ability to form blue plaques in a Bluo-gal overlay. Blue plaques were plaque purified three times before stocks were prepared. The VP5 and VP23 mutants were designated K5ΔZ and K23Z, respectively. To confirm the introduction of the *lacZ* gene into these viruses, small batches of viral DNA were prepared from infected cells and analyzed by Southern blot hybridization. Results of this experiment are shown in Fig. 3. In the case of K5ΔZ, a deletion of 1.8 kb was created, followed by addition of the 3-kb *lacZ* fragment. This resulted in an overall insertion of 1.2 kb. Digestion of viral DNA with *Bgl*II resulted in the appearance of a band corresponding to the 5.7-kb *Bgl*II N fragment in KOS DNA (lane 3), and this increased in size to 6.9 kb in the K5ΔZ digest (lane 4). The presence of an *Eco*RI site in the *lacZ* gene resulted in cleavage of the *Eco*RI G fragment (16.2 kb) of KOS (lane 1) into 9.4- and 8-kb fragments in the mutant (lane 2). KOS DNA restricted with *Stu*I and *Sal*I give rise to bands that were 4.3 (lane 5) and 3.3 (lane 7) kb in size, respectively. These fragments both increased in size by 3 kb in the K23Z digest (lanes 6 and 8), owing to insertion of the *lacZ* gene.

TABLE 2. Plating efficiency of viruses on transformed cells

Virus	Plating efficiency (PFU/ml) on:		
	Vero	E43	G5
KOS	2.6×10^{10}	1.9×10^{10}	2.4×10^{10}
K5ΔZ	7×10^{5}	6.7×10^{9}	1.03×10^{10}
K23Z	3×10^{6}	2.9×10^{6}	1.51×10^{10}

Phenotypic characterization of the mutants. The plating efficiency of the viruses was tested on different cell lines to further confirm the genotype of these mutants. Stocks of the mutant viruses prepared in G5 cells were plated on monolayers of either Vero, E43, or G5 cells. The results of this assay are shown in Table 2. As expected, both mutants gave rise to plaques on G5 monolayers, and only K5ΔZ formed plaques on E43 cells (transformed with only the *Bgl*II-N sequence). The levels of wild-type virus in the mutant stocks represent recombination between homologous DNA sequences present in the mutant virus genomes and in the chromosome of the transformed cell line. The percentages of wild-type virus in K5ΔZ and K23Z stocks were 0.007 and 0.02%, respectively. Similar results have been obtained with other independent stocks of these viruses.

The next series of experiments was carried out to confirm the absence of either VP5 or VP23 in extracts from mutant-infected nonpermissive cells. Vero and G5 cells were infected with KOS, K5ΔZ, and K23Z at an MOI of 10 PFU per cell and metabolically labelled with [^{35}S]methionine from 9 to 24 h postinfection. Total infected-cell polypeptides were examined by SDS-PAGE (Fig. 4A). Results are shown for KOS-, K5ΔZ-, and K23Z-infected Vero (lanes 2 through 4) and G5 (lanes 6 through 8) cells, respectively. Both K5ΔZ (lane 3) and K23Z (lane 4) synthesized wild-type levels of infected-cell proteins under nonpermissive conditions. However, the band corresponding to the 150-kDa VP5 protein was absent in K5ΔZ lysates and the 33-kDa band corresponding to VP23 was absent in K23Z lysates (arrowheads). These proteins were present in lysates prepared from mutant-infected G5 cells (lanes 7 and 8), albeit at lower levels. Apparently, the expression of VP5 and VP23 from the integrated copy of *Eco*RI-G in G5 cells is lower than expression of these proteins from the wild-type virus. Expression of VP23 in K5ΔZ was increased relative to its expression in KOS (compare lanes 2 and 3). The reason for this is unclear. The same protein lysates were reacted with either a monoclonal antibody to VP5 (LP12) or a polyclonal rabbit serum raised against VP23 (CP3). Immunoprecipitates were analyzed by SDS-PAGE, the results of which are shown in Fig.

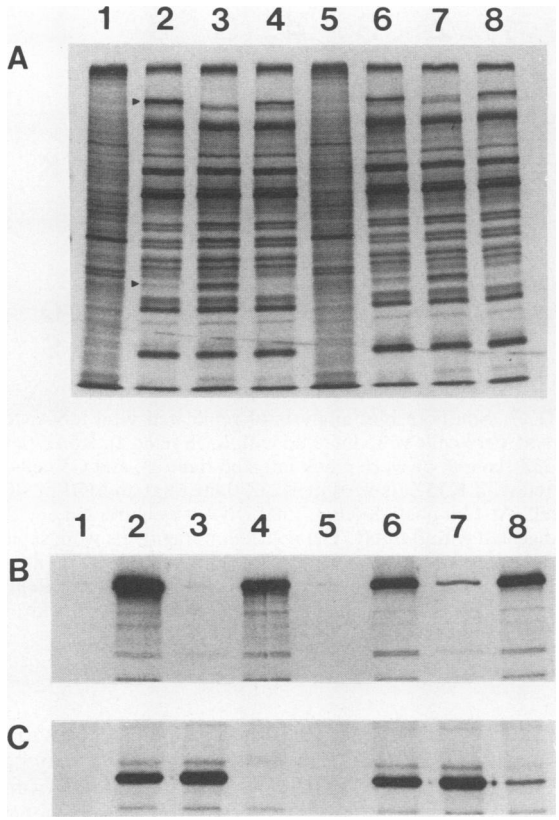

FIG. 4. Synthesis of viral polypeptides in K5ΔZ- and K23Z-infected cells. Vero (lanes 1 to 4) and G5 (lanes 5 to 8) cells were infected at an MOI of 10 PFU per cell with KOS (lanes 2 and 6), K5ΔZ (lanes 3 and 7), or K23Z (lanes 4 and 8) or were mock infected (lanes 1 and 5). Cells were metabolically labelled with [^{35}S]methionine from 9 to 24 h after infection. Lysates prepared from the cells were subjected to SDS–12% PAGE (panel A) or precipitated with antibody LP12 (VP5) (panel B) or CP3 (VP23) (panel C), and the resulting immunoprecipitates were analyzed by SDS–12% PAGE.

4B and C. The results of the immunoprecipitation assay further confirm these findings.

Ultrastructural analysis of mutant-infected cells. The VP5 and VP23 null mutants were examined by electron microscopy to determine whether they form mature capsids or accumulate visible capsid precursors under nonpermissive conditions. Mutant and parental viruses were used to infect permissive and nonpermissive cells, and the nuclei in tissue sections were examined by electron microscopy. Samples were fixed in glutaraldehyde at 12, 18, and 24 h after infection. Results of the 12-h infection are shown in Fig. 5. Capsids were detected in KOS-infected Vero cells (A) and in G5 cells infected with K5ΔZ (B) or K23Z (E). No capsid-like structure was observed in Vero cells infected with either K5ΔZ (C) or K23Z (F). The nuclei of the mutant-infected Vero cells appeared to be similar to those of mock-infected Vero cells (D), except for the condensation of chromatin material, a feature characteristic of infected cells. Most of the tissue slices showed capsids in preparations of K5ΔZ- and K23Z-infected G5 cells or in KOS-infected Vero cells. However, no capsids were observed for approximately 30 sections each of the mutant-infected Vero cells.

Sedimentation analysis of mutants. The absence of mature capsids in Vero cells infected with K5ΔZ and K23Z does not preclude the existence of capsid precursors which may accumulate in these cells. Therefore, nuclear extracts of mutant-infected cells were analyzed by sedimentation through sucrose gradients. HEL cells were used as the

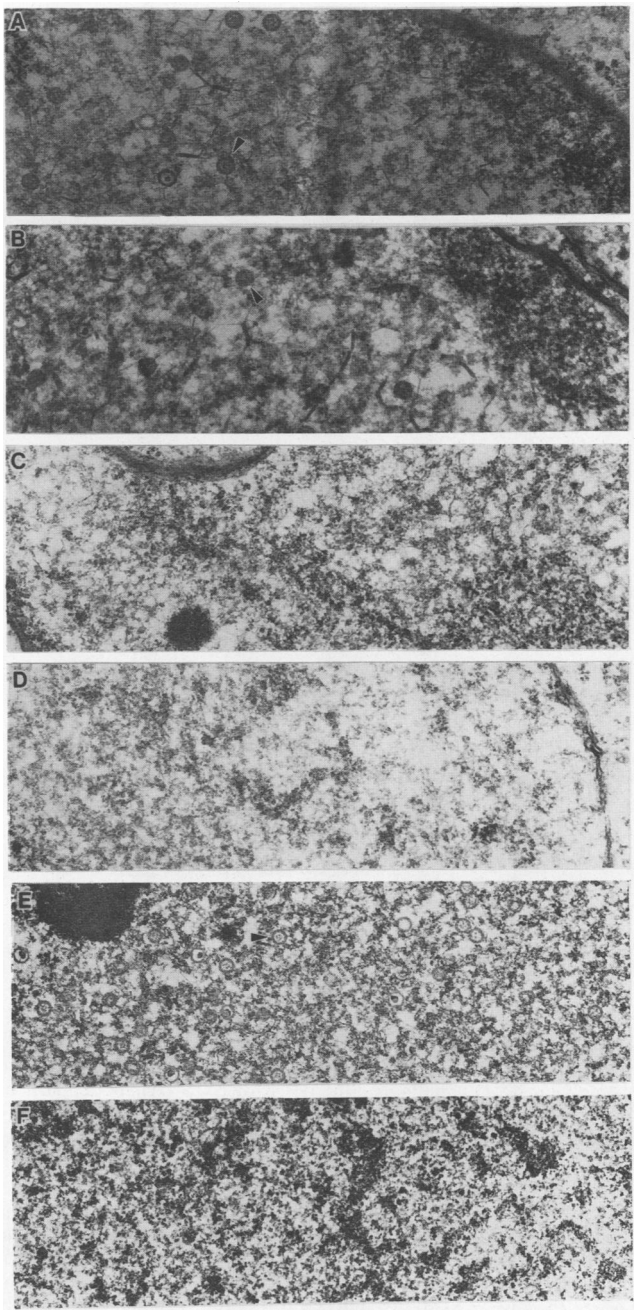

FIG. 5. Electron micrographs of thin sections of infected cells. Monolayers of Vero cells were infected with KOS (A), K5ΔZ (C), or K23Z (F) or were mock infected (D), and G5 cells were infected with K5ΔZ (B) or K23Z (E) at an MOI of 10 PFU per cell. At 12 h postinfection, cells were fixed in 2.5% glutaraldehyde in phosphate-buffered saline and embedded in Scipoxy 812 resin, and 50- to 70-nm-thick sections prepared for examination in a JEOL 100 CX electron microscope. Electron microscopic analysis was performed at the Structural Biology Center, University of Pittsburgh. Magnifications were ×27,750 for panels A to D and ×25,900 for panels E to F. Capsids are marked with arrowheads.

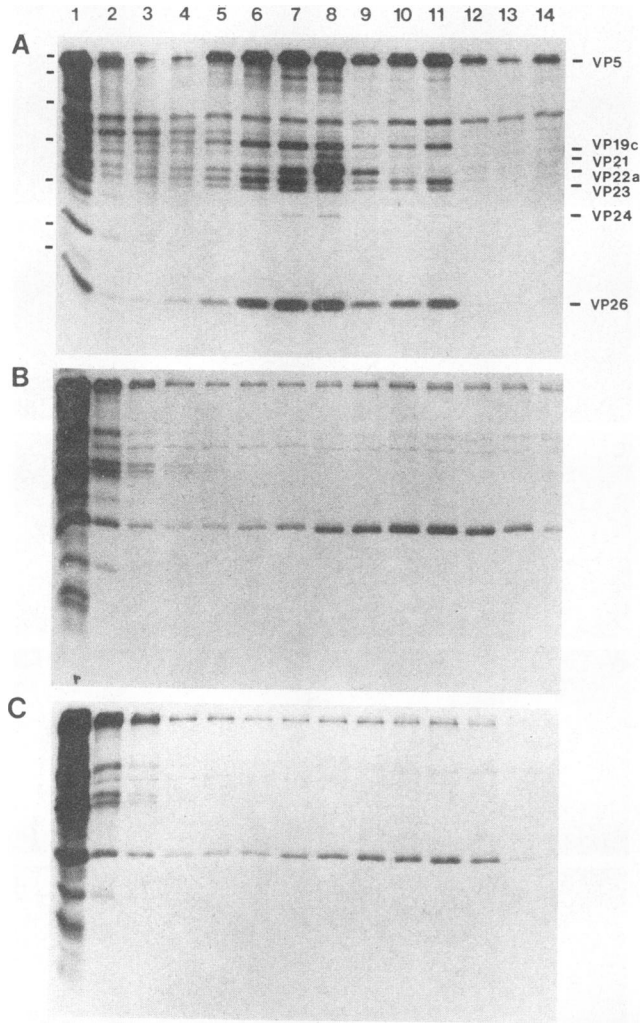

FIG. 6. Sedimentation analysis of nuclear lysates from infected HEL cells. HEL cells were infected with KOS (A), K5ΔZ (B), or K23Z (C) at an MOI of 10 PFU per cell. Cells were metabolically labelled with [^{35}S]methionine from 6 to 12 h postinfection. Nuclear lysates were layered onto 20 to 50% sucrose gradients and sedimented at 24,000 rpm for 100 min in a Beckman SW41 rotor. Fractions were collected, and proteins were analyzed by SDS–17% PAGE. The direction of sedimentation is from left to right. The mobilities of the seven capsid proteins are marked. The positions of protein standards in order of decreasing molecular mass (200, 97, 68, 43, 29, 18, and 14 kDa) are marked to the left of panel A.

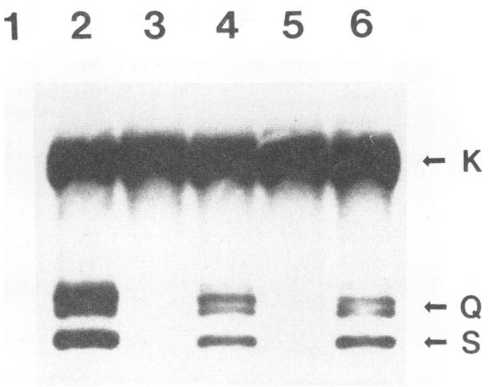

FIG. 7. Southern blot analysis of replicated viral DNA. Monolayers of Vero cells were infected with KOS (lane 2), K5ΔZ (lane 3), or K23Z (lane 5) or were mock infected (lane 1), and G5 cells were infected with K5ΔZ (lane 4) or K23Z (lane 6) at an MOI of 10 PFU per cell. At 12 h postinfection, total DNA was extracted and 2.5 μg was digested with *Bam*HI. The restriction fragments were separated on a 1% agarose gel and transferred to nitrocellulose. The filter was hybridized to a ^{32}P-labelled probe corresponding to *Bam*HI-K sequences. The junction, K (5.9 kb), and terminal, Q (3.4 kb) and S (3.0 kb), fragments are indicated.

nonpermissive cell line. Cell monolayers were infected with KOS or the mutant viruses and labelled with [^{35}S]methionine from 6 to 12 h postinfection. Nuclear lysates were prepared and layered onto 20 to 50% sucrose gradients. After sedimentation, fractions were collected and analyzed by SDS-PAGE (Fig. 6). Fraction 1, at the left of Fig. 6, corresponds to the top of the centrifuge tube. Two peaks of radioactivity were observed for KOS-infected cells (Fig. 6A), corresponding to the faster-sedimenting C capsids (fraction 11) and the empty B capsids (fractions 6 through 8). Both B and C capsids contained VP5, VP19c, VP23, VP24, and VP26. VP22a and, perhaps, VP21 were detected only in B capsids, as expected. We believe that the double band of radioactivity migrating at 33 to 37 kDa represents different phosphorylated forms of VP23. VP23 in the virion has been shown to be phosphorylated (17). This processing activity may be cell type dependent, since VP23 in capsids isolated from the nuclei of Vero cells migrates as a single band. Sedimentation analysis of the mutant lysates (Fig. 6B and C) revealed no cosedimenting capsid proteins in any of the fractions. Presumably, all of the capsid proteins were at the top of the gradient. Bands with mobilities corresponding to approximately 150 and 30 kDa appeared in all of the fractions for all of the virus-infected cells and therefore do not correspond to capsid proteins.

Viral DNA analysis. Viral DNA analysis experiments were carried out to determine the state of viral DNA in nonpermissive cells infected with the VP5 and VP23 mutants. Both mutants failed to form mature capsids or capsid-like structures upon infection of Vero cells. Nevertheless, the proteins required for replication, processing, and packaging of viral DNA are presumably expressed in both mutants. Southern blot analysis was carried out to determine the level of viral DNA replication and the processing of replicated DNA into unit length molecules in the absence of capsid structures. Vero and G5 cells were infected with KOS, K5ΔZ, and K23Z. Infected-cell DNA was extracted and analyzed by Southern blot hybridization by using the *Bam*HI K junction fragment as a probe (Fig. 7). In DNAs extracted from KOS-infected Vero cells (lane 2) and G5 cells infected with K5ΔZ (lane 4) and K23Z (lane 6), the K junction fragment and the two end, Q and S, fragments were detected by hybridization, a result consistent with the presence of linear unit length genomes. The presence of multiple bands of Q is due to the heterogeneity of *a* sequences at that end of the genome. Only the junction fragment was observed in DNA extracted from Vero cells infected with K5ΔZ (lane 3) or K23Z (lane 5). Therefore, in the absence of VP5 or VP23 and, consequently, mature capsids, high-molecular-weight viral DNA is not processed into unit length molecules. The amount of the junction fragment detected and, therefore, the extent of DNA replication are the same for mutant- and wild-type-infected cells.

DISCUSSION

The ability to construct transformed cell lines that express a gene in *trans* has enabled the isolation of null mutations in essential genes of HSV-1. We have isolated Vero cell lines transformed with sequences that express VP5 alone (E43) or both VP5 and VP23 (G5). These cell lines were selected for by virtue of their ability to plaque *ts*1178, a *ts* mutant in VP5, at the nonpermissive temperature. Null mutants were generated in the genes for VP5 (*UL19*) and VP23 (*UL18*) by insertion of *lacZ* sequences at codons 1 and 11, respectively. These were transferred into the KOS genome by homologous recombination by using transformed Vero cells as the permissive line. Both the VP5 (K5ΔZ) and VP23 (K23Z) mutants failed to replicate on Vero cells. Therefore, VP23, like VP5, is an essential gene product. Only K5ΔZ replicated on the cell line transformed with only the *UL19* sequences. The absence of expression of the VP5 and VP23 polypeptides in the respective mutants was confirmed by SDS-PAGE analysis of protein lysates and immunoprecipitation with antibodies specific for these proteins. Both mutants expressed wild-type levels of infected-cell polypeptides under nonpermissive conditions. Interestingly, expression of VP23 in K5ΔZ was increased relative to wild-type levels. The reason for this is unclear. The null mutants were unable to assemble capsids upon infection of nonpermissive cells, as judged by electron microscopic analysis of thin sections. By using sedimentation analysis of nuclear extracts prepared from KOS-infected cells, B and C capsids were detected. However, for either the VP5 or the VP23 mutant, no capsid structures were observed in the gradient at positions where wild-type capsids sediment.

The amount of DNA replication is normal in K5ΔZ- and K23Z-infected nonpermissive cells, but the DNA exists as concatemers that are not processed to genome length molecules. Normally during viral replication, concatemers are cleaved into unit length genomes, presumably at the time of encapsidation. It appears that if viral DNA is not packaged into capsids it is not cleaved (27, 32). In addition to null mutants for capsid genes that specify VP5 and VP23, *ts* mutations in VP19c and VP22a also result in accumulation of concatemeric DNA (26, 27). Unlike the other three capsid proteins, VP22a is found in empty but not in DNA-filled capsids (33, 38). In addition to the capsid components, *ts* mutations that produce the same DNA-processing phenotype have been identified in five additional genes (1–3, 32). Therefore, capsid formation is necessary, but not sufficient, for cleavage of DNA into head-full lengths. While one of the noncapsid proteins may possess enzyme activity for site-specific cleavage, the requirement of five gene products is puzzling. Since DNA cleavage is linked to packaging, it is also surprising that one or more of these proteins have not been detected as capsid-binding proteins.

The HSV-1 capsid is a complex structure composed of up to seven proteins, each of which is important for assembly of the mature capsid, which is then incorporated into the virion. The steps that occur in the assembly of capsids have not been elucidated. The isolation of mutations in each of the seven capsid gene products should enable one to identify the steps involved in capsid assembly and the role of each protein in that pathway. *ts* lesions have been the primary source of mutations in the capsid genes, and these have been used to characterize the roles of VP5, VP19c, and VP22a in capsid morphogenesis. Lesions in VP22a result in synthesis of viral DNA and empty capsids; however, DNA packaging is defective in these mutants (27, 38). *ts* mutations in VP5 (41) and VP19c (26) result in lack of mature capsid formation; nevertheless, small ring-like structures were observed by electron microscopic analysis of cells infected with *ts*1178 (VP5) at the nonpermissive temperature (30). It is not clear whether this latter result is due to leakiness in the *ts* phenotype or a real precursor in the capsid assembly pathway. To overcome problems of leakiness in the *ts* phenotype, null mutants need to be isolated so that the role of each gene can be defined in its complete absence. To this end, we have isolated null mutants for two important capsid proteins, VP5 and VP23. We have not detected any structure that resembles capsid precursors in infected cells. However, these studies require sedimentation parameters different from those employed for complete capsids (20 to 50% sucrose gradients) and the experimental conditions, i.e., the salt concentration, may have to be varied to stabilize interactions between capsid molecules. The absence of large macromolecular structures in the sucrose gradients shown here does indicate that VP5 and VP23 play a major role in the assembly of capsids.

ACKNOWLEDGMENTS

This work was supported by Public Health Service grants from the National Institutes of Health.

We thank Brendon Wahlberg for preparation of figures.

REFERENCES

1. **Addison, C., F. J. Rixon, J. W. Palfreyman, M. O'Hara, and V. G. Preston.** 1984. Characterization of a herpes simplex virus type 1 mutant which has a temperature-sensitive defect in penetration of cells and assembly of capsids. Virology **138**:246–259.
2. **Addison, C., F. J. Rixon, and V. G. Preston.** 1990. Herpes simplex virus type 1 UL28 gene is important for the formation of mature capsids. J. Gen. Virol. **71**:2377–2384.
3. **Al-Kobaisi, M. F., F. J. Rixon, I. McDougall, and V. G. Preston.** 1991. The herpes simplex virus UL33 gene product is required for the assembly of full capsids. Virology **180**:380–388.
4. **Baker, T. S., W. W. Newcomb, F. P. Booy, J. C. Brown, and A. C. Steven.** 1990. Three-dimensional structures of maturable and abortive capsids of equine herpesvirus 1 from cryoelectron microscopy. J. Virol. **64**:563–573.
5. **Booy, F. P., W. W. Newcomb, B. L. Trus, J. C. Brown, T. S. Baker, and A. C. Steven.** 1991. Liquid-crystalline, phage-like packing of encapsidated DNA in herpes simplex virus. Cell **64**:1007–1015.
6. **Braun, D. K., W. Batterson, and B. Roizman.** 1984. Identification and genetic mapping of a herpes simplex virus capsid protein that binds DNA. J. Virol. **50**:645–648.
7. **Cai, W., S. Person, C. DebRoy, and B. Gu.** 1988. Functional regions and structural features of the gB glycoprotein of herpes simplex virus type 1: an analysis by linker insertion mutants. J. Mol. Biol. **201**:575–588.
8. **Chakrabarti, S., K. Brechling, and B. Moss.** 1985. Vaccinia virus expression vector: co-expression of β-galactosidase provides a visual screening of recombinant plaques. Mol. Cell. Biol. **5**:3403–3409.
9. **Cohen, G. H., M. Ponce de Leon, H. Diggleman, W. C. Lawrence, S. K. Vernon, and R. J. Eisenberg.** 1980. Structural analysis of the capsid polypeptides of herpes simplex virus types 1 and 2. J. Virol. **34**:521–531.
10. **Costa, R. H., G. Cohen, R. Eisenberg, D. Long, and E. Wagner.** 1984. Direct demonstration that the abundant 6-kilobase herpes simplex virus type 1 mRNA mapping between 0.23 and 0.27 map units encodes the major capsid protein VP5. J. Virol. **49**:287–292.
11. **DeLuca, N. A., A. M. McCarthy, and P. A. Schaffer.** 1985. Isolation and characterization of deletion mutants of herpes simplex virus type 1 in the gene encoding immediate-early regulatory protein ICP4. J. Virol. **56**:558–570.

12. **Feinberg, A. P., and B. Vogelstein.** 1984. A technique for radiolabelling DNA restriction fragments to high specific activity. Anal. Biochem. **137**:6–13.
13. **Furlong, D.** 1978. Direct evidence for 6-fold symmetry of the herpesvirus hexon capsomers. Proc. Natl. Acad. Sci. USA **75**:2764–2766.
14. **Gibson, W., and B. Roizman.** 1972. Proteins specified by herpes simplex virus. VIII. Characterization and composition of multiple capsid forms of subtypes 1 and 2. J. Virol. **10**:1044–1052.
15. **Graham, F. L., and A. J. Van der Eb.** 1973. A new technique for the assay of infectivity of human adenovirus 5 DNA. Virology **52**:456–467.
16. **Heilman, C. J., Jr., M. Zweig, J. R. Stephenson, and B. Hampar.** 1979. Isolation of a nucleocapsid polypeptide of herpes simplex virus types 1 and 2 possessing immunologically type-specific and cross-reactive determinants. J. Virol. **29**:34–42.
17. **Lemaster, S., and B. Roizman.** 1980. Herpes simplex virus phosphoproteins. II. Characterization of the virion protein kinase and of the polypeptides phosphorylated in the virion. J. Virol. **35**:798–811.
18. **Liu, F., and B. Roizman.** 1991. The promoter, transcriptional unit, and coding sequences of herpes simplex virus 1 family 35 proteins are contained within and in frame with the UL26 open reading frame. J. Virol. **65**:206–212.
19. **Liu, F. Y., and B. Roizman.** 1991. The herpes simplex virus type 1 gene encoding a protease also contains within its coding domain the gene encoding the more abundant substrate. J. Virol. **65**:5149–5156.
20. **McGeoch, D. J., M. A. Dalrymple, A. J. Davison, A. Dolan, M. C. Frame, D. McNab, L. J. Perry, J. E. Scott, and P. Taylor.** 1988. The complete DNA sequence of the long unique region in the genome of herpes simplex virus type 1. J. Gen. Virol. **69**:1531–1574.
21. **McGeoch, D. J., S. K. Weller, and P. A. Schaffer.** 1990. Herpes simplex virus, p. 1.115–1.120. *In* S. J. O'Brien (ed.), Genetic maps, Cold Spring Harbor Laboratory Press, Cold Spring Harbor, N.Y.
22. **Newcomb, W. W., and J. C. Brown.** 1989. Use of Ar^+ plasma etching to localize structural proteins in the capsid of herpes simplex virus type 1. J. Virol. **63**:4697–4702.
23. **Newcomb, W. W., and J. C. Brown.** 1991. Structure of the herpes simplex virus capsid: effects of extraction with guanidine hydrochloride and partial reconstitution of extracted capsids. J. Virol. **65**:613–620.
24. **Newcomb, W. W., J. C. Brown, F. P. Booy, and A. C. Steven.** 1989. Nucleocapsid mass and capsomer protein stoichiometry in equine herpes virus type 1: a scanning transmission electron microscopic study. J. Virol. **63**:3777–3783.
25. **Person, S., R. W. Knowles, G. S. Read, S. C. Warner, and V. C. Bond.** 1976. Kinetics of cell fusion induced by a syncytia [sic]-producing mutant of herpes simplex virus type 1. J. Virol. **17**:183–190.
26. **Pertuiset, B., M. Boccara, J. Cebrian, N. Berthelot, S. Chousterman, F. Puvion-Dutilleul, J. Sisman, and P. Sheldrick.** 1989. Physical mapping and nucleotide sequence of a herpes simplex virus type 1 gene required for capsid assembly. J. Virol. **63**:2169–2179.
27. **Preston, V. G., J. A. V. Coates, and F. J. Rixon.** 1983. Identification and characterization of a herpes simplex virus gene product required for encapsidation of virus DNA. J. Virol. **45**:1056–1064.
28. **Preston, V. G., F. J. Rixon, I. M. McDougall, M. McGregor, and M. F. Al Kobaisi.** 1992. Processing of the herpes simplex virus assembly protein ICP35 near its carboxy terminal end requires the product of the whole of the UL26 reading frame. Virology **186**:87–98.
29. **Schaffer, P. A., G. M. Aron, N. Biswal, and M. Benyesh-Melnick.** 1973. Temperature-sensitive mutants of herpes simplex virus type 1: isolation, complementation and partial characterization. Virology **52**:57–71.
30. **Schaffer, P. A., J. P. Brunschwig, R. M. McCombs, and M. Benyesh-Melnick.** 1974. Electron microscopic studies of temperature-sensitive mutants of herpes simplex virus type 1. Virology **62**:444–457.
31. **Schrag, J. D., B. V. V. Prasad, F. J. Rixon, and W. Chiu.** 1989. Three-dimensional structure of the HSV-1 nucleocapsid. Cell **56**:651–660.
32. **Sherman, G., and S. L. Bachenheimer.** 1987. DNA processing in temperature-sensitive morphogenic mutants of HSV-1. Virology **158**:427–430.
33. **Sherman, G., and S. L. Bachenheimer.** 1988. Characterization of intranuclear capsids made by ts morphogenic mutants of HSV-1. Virology **163**:471–480.
34. **Southern, E. M.** 1975. Detection of specific sequences among DNA fragments separated by gel electrophoresis. J. Mol. Biol. **98**:503–517.
35. **Southern, P. J., and P. Berg.** 1982. Transformation of mammalian cells to antibiotic resistance with a bacterial gene under the control of the SV40 early region promoter. J. Mol. Appl. Genet. **1**:327–341.
36. **Steven, A. C., C. R. Roberts, J. Hay, M. E. Bisher, M. Pun, and B. L. Trus.** 1986. Hexavalent capsomers of herpes simplex virus type 2: symmetry, shape, dimensions, and oligomeric status. J. Virol. **57**:578–584.
37. **Stow, N., and N. M. Wilkie.** 1976. An improved technique for obtaining enhanced infectivity with herpes simplex virus type 1 DNA. J. Gen. Virol. **33**:447–458.
38. **Rixon, F. J., A. M. Cross, C. Addison, and V. G. Preston.** 1988. The products of the herpes simplex virus type 1 gene UL26 which are involved in DNA packaging are strongly associated with empty but not with full capsids. J. Gen. Virol. **69**:2879–2891.
39. **Rixon, F. J., M. D. Davison, and A. J. Davison.** 1990. Identification of the genes encoding two capsid proteins of herpes simplex virus type 1 by direct amino acid sequencing. J. Gen. Virol. **71**:1211–1214.
40. **Vernon, S. K., M. Ponce de Leon, G. H. Cohen, R. J. Eisenberg, and B. A. Rubin.** 1981. Morphological components of herpesvirus. III. Localization of herpes simplex virus type 1 nucleocapsid polypeptides by immune electron microscopy. J. Gen. Virol. **54**:39–46.
41. **Weller, S. K., E. P. Carmichael, D. P. Aschman, D. J. Goldstein, and P. A. Schaffer.** 1987. Genetic and phenotypic characterization of mutants in four essential genes that map to the left half of HSV-1 UL DNA. Virology **161**:198–210.
42. **Wildy, P., W. C. Russell, and R. W. Horne.** 1960. The morphology of herpes virus. Virology **12**:204–222.
43. **Zweig, M., C. J. Heilman, and B. Hampar.** 1979. Identification of disulfide-linked protein complexes in the nucleocapsids of herpes simplex virus type 2. Virology **94**:442–450.